Multi-user interference characterization in antenna arrays: an algebraic angle approach

Mohammed Reda Bekkar, Laurent Ros, Cyrille Siclet, Serge Bories, Benoit Miscopein

Multi-user interference characterization in antenna arrays: an algebraic angle approach.

M. R. Bekkar, L. Ros, C. Siclet, S. Bories, B. Miscopein

Antenna arrays are widely used in radar systems and mobile networks in the physical layer to mitigate interference as well as to enhance the reliability and the capacity of the system. The performance of beamforming algorithms depends on the channel realization and its associated micro-parameters (angle of arrivals, multi-path components, fading) plus the array geometry. The multiplicity of these micro-parameters makes it difficult to establish a tractable characterization of the overall performance. In this paper, a new parameter, an algebraic angle cosine between the signal subspace and the interference subspace, is introduced to characterize the interference impact. It allows the derivation of a lower bound on the signal-to-interference-plus noise ratio (SINR) of the Capon beamformer. Outside two regions where the interferers are quasi-orthogonal or quasi-aligned with the desired user, the lower bound decreases linearly with this parameter.

Introduction: The data-rate provided by wireless communications is in increasing demand as the mobile networks evolve. Not only are the number of users on the rise, but the density of base stations deployed is increasing. As a result, service providers and equipment manufacturers face interference issues associated with this densification [1]. For instance, in 5G networks antenna array systems are one of the key enablers to manage interference and improve the system overall performance [2]. In this context various interference cancellation algorithms exist, and the Capon beamformer [3] is a well-known and studied solution for this purpose [4, 5]. In terms of signal-to-interference-plus-noise ratio (SINR), it attains the optimal value. From an overall perspective, the performance of beamforming algorithms depends on the spatial channels and the statistical distribution of its micro-parameters, i.e. the array geometry, the presence of multi-path components, angle of arrival statistics and fading. This makes the characterization of the performances conditioned to the channel model [6, 7] and its configuration. In general, the contribution of each of the micro-components to the overall behavior of a macro-parameter (SINR for e.g.) is dependent on the characteristics of each component. In this paper, a new channel macro-parameter that characterizes the interference in terms of algebraic angle cosine ($\cos(\theta)$) is presented. The algebraic angle considered, θ, is between the signal subspace and the interference subspace. In the single-interferer case, the parameter allows determination of the SINR attained by the Capon beamformer. In the multi-interferer case, it allows the determination of a lower bound on the SINR. Results from experiment support the existence of a closed form relationship between SINR and the algebraic macro properties. The macro-parameter (SINR) can be calculated or predicted using the derived theoretical relationship through the use of the proposed $\cos(\theta)$ macro-parameter. The system model is presented first along with the parameter definition for the single-interferer case, and then its generalization to the multi-interferer case. After that an application on TDD (Time Division Duplexing) dense small cell network scenario is given.

Notations: Capital boldface characters are used to note matrices, and lower case boldface characters are used to note column vectors. $(\cdot)^H$, $(\cdot)^{-1}$ denote the conjugate transpose and the matrix inverse respectively. The (k)-th column of a matrix $\mathbf{A}$ is noted $\mathbf{a}_{(k)}$. $\propto$ stands for proportional to. $\mathrm{Span}(\mathbf{A})$ stands for the subspace linearly spanned by a matrix $\mathbf{A}$. $[\mathbf{A}|\mathbf{B}]$ corresponds to the column-wise concatenation of two matrices $\mathbf{A}$ and $\mathbf{B}$.

System Model:

Single-User Single-Interferer Model

Assume that a signal of a user x_U and an interferer signal x_I are received by an n_r antenna array. If the signals are narrow-band the complex envelope of the array output can be modeled as [8]:

$$\mathbf{y} = \mathbf{h}_U x_U + \mathbf{h}_I x_I + \mathbf{n} \tag{1}$$

where $\mathbf{y}$, $\mathbf{n}$, $\mathbf{h}_U$ and $\mathbf{h}_I$ are the received signal vector, the thermal noise vector, the user channel vector and the interferer channel vector respectively; all of them taken in $\mathbb{C}^{n_r}$. For a given channel realization, the conventional Capon beamformer $\mathbf{w}_C$ is known to maximize the SINR and is proportional to:

$$\mathbf{w}_C = \underset{\mathbf{w}}{\mathrm{argmax}} \quad \frac{\mathbf{w}^H \mathbf{R}_U \mathbf{w}}{\mathbf{w}^H(\mathbf{R}_I + \mathbf{R}_\mathbf{n})\mathbf{w}} \propto (\mathbf{R}_I + \mathbf{R}_\mathbf{n})^{-1}\mathbf{h}_U \tag{2}$$

where $\mathbf{R}_U = \sigma_U^2 \mathbf{h}_U \mathbf{h}_U^H$, $\mathbf{R}_I = \sigma_I^2 \mathbf{h}_I \mathbf{h}_I^H$ and $\mathbf{R}_\mathbf{n} = \sigma_n^2 \mathbf{I}$ are the user, interferer and thermal noise autocorrelation matrices respectively. The SINR output of the filter is:

$$\mathrm{SINR} = \frac{\mathbf{w}_C^H \mathbf{R}_U \mathbf{w}_C}{\mathbf{w}_C^H(\mathbf{R}_I + \mathbf{R}_\mathbf{n})\mathbf{w}_C} \tag{3}$$

Since the SINR is a generalized Rayleigh quotient, it can be shown that the SINR value attained by the Capon beamformer is equal to the only non-zero eigenvalue of the matrix $(\mathbf{R}_I + \mathbf{R}_\mathbf{n})^{-1}\mathbf{R}_U$. There is only one non-zero eigenvalue since $\mathrm{rank}(\mathbf{R}_U) = 1$. This eigenvalue depends on the channel realization, the array geometry and the angles of arrival. Its maximum possible value is $n_r.\mathrm{SNR}$, where:

$$n_r \mathrm{SNR} = n_r \frac{\sigma_U^2}{\sigma_n^2} \quad \text{(Capon SINR Best Case)} \tag{4}$$

this value is attained in the case of no interference or perfect interference cancellation. On the other hand, its minimum possible value is:

$$\mathrm{SINR_{in}} = \frac{\sigma_U^2}{\sigma_I^2 + \sigma_n^2} \quad \text{(Capon SINR Worst Case)} \tag{5}$$

this value is attained if $\mathbf{h}_I \propto \mathbf{h}_U$. For fixed signal power, this eigenvalue (and then the Capon SINR) varies between these extrema, and depends of the angles of arrivals. This dependence is multi-dimensional in the presence of multi-path and becomes intractable to characterize in the multi-user multi-interferer case. Thus, the following algebraic angle cosine parameter is introduced to characterize the interference. In the single-user single-interferer case it is expressed as:

$$|\cos(\theta)| = \frac{|\mathbf{h}_I^H \mathbf{h}_U|}{||\mathbf{h}_I||.||\mathbf{h}_U||} \tag{6}$$

Please note that the angle θ is different from the physical angles of arrivals, and $|\cos(\theta)|$ corresponds to the correlation coefficient between the user and the interferer channel vectors. If the array is uniformly linear (ULA) and the channel is single-path it can be linked to the angles or arrivals [8]:

$$|\cos(\theta)| = \left| \frac{1}{n_r} . \frac{\sin\left(n_r \pi d(\sin(\phi_I) - \sin(\phi_U))\right)}{\sin\left(\pi d(\sin(\phi_I) - \sin(\phi_U))\right)} \right| \tag{7}$$

where ϕ_I, ϕ_U and d are the interferer angle of arrival, the user angle of arrival and the inter-antenna distance relative to the wavelength respectively.

Multi-User Multi-Interferer Model

The previous model can easily be generalized to the case with n_U users and n_I interferers by stacking the channel vectors into the matrices $\mathbf{H}_U$ and $\mathbf{H}_I$ of sizes $n_r \times n_U$ and $\mathbf{n}_r \times n_I$ respectively, and by stacking the signals into the vectors $\mathbf{x}_U$ and $\mathbf{x}_I$:

$$\mathbf{y} = \mathbf{H}_U \mathbf{x}_U + \mathbf{H}_I \mathbf{x}_I + \mathbf{n} \tag{8}$$

In this case, the algebraic angle cosine between one desired user u and the hyper-plane generated by the $(n_U - 1)$ other users and the n_I interferers is defined as:

$$|\cos(\theta_u)| = \max_{\mathbf{h}_i} \frac{|\mathbf{h}_i^H \mathbf{h}_u|}{||\mathbf{h}_i||.||\mathbf{h}_u||}, \quad \mathbf{h}_i \in \mathrm{Span}([\mathbf{H}_{\bar{U}}|\mathbf{H}_I]) \tag{9}$$

where $\mathbf{H}_{\bar{U}}$ is formed by removing the u-th columns from $\mathbf{H}_U$. Fig. 1 illustrates this angle in the case of two antennas and two interferers. Computing this angle cosine requires solving the optimization problem (9), numerical solutions exist [9, 10] and are implemented for instance in the function `subspace` of Matlab.

Application and Results: In this section, the relevance of the algebraic angle for the analysis of the SINR is illustrated in two cases, first in a deterministic single-user single-interferer case, and then for small cell network case with random positions. For the sake of simplicity, the results for a ULA single-path channel are shown, but their generalization is straightforward for the multi-path non-frequency selective channel with arbitrary array geometry.

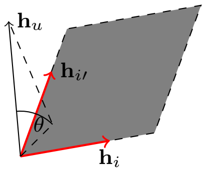

Fig. 1: Algebraic angle illustration. $n_r = 3$, $n_I = 2$.

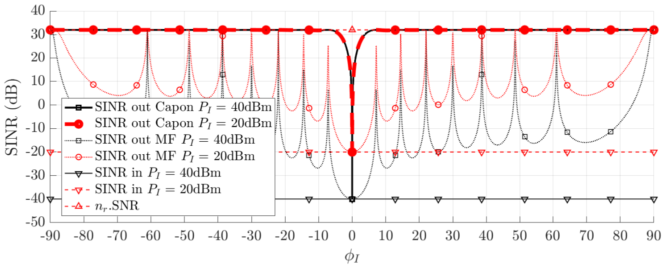

Fig. 2: Single-user single-interferer SINR as a function of ϕ_I.

Single-User Single-Interferer Case

Consider a receiving array with $n_r = 16$ antennas, a user located at the direction $\phi_U = 0°$ and an interferer with a varying direction of arrival in $\phi_I \in [-90°, 90°]$. The user power is fixed to 0 dBm, the interferer power $P_I \in \{20, 40\}$dBm and the SNR = 20dB. The channel model considered is thus deterministic. The variation of the SINR obtained from eq. (3) is plotted on Fig. 2. The variation is between the extremal values SINR_{in} and n_r.SNR. In a large region the maximum value n_r.SNR is attained, except around the tight region where $\phi_I \simeq \phi_U$. For purposes of comparison, also plotted is the SINR attained by the matched filter and noticed is that it has high losses in comparison with the Capon. In Fig. 3 the variation of the $|\cos(\theta)|$ parameter using eq. (7) in the same conditions is plotted. In this simple case the plot resembles a radiation pattern that narrows as the number of antenna increases. It achieves its highest values in the main lobe area. Notice that in this main lobe area the SINR drops drastically. Subsequently, the focus is made on how this parameter conditions the SINR. Plotted in Fig. 4 is the SINR as a function of $|\cos(\theta)|$, obtained by combining the two previous figures. This shows a bijective relation between the SINR and $|\cos(\theta)|$. The region around $|\cos(\theta)| \simeq 1$ is of special interest since it is around that the performance drops. Fig. 5 expands this region using $1 - |\cos(\theta)|$ with a log scale. The main lobe area ($\cos(\theta) \simeq 1$) corresponds to the values of $1 - |\cos(\theta)| \simeq 0$, i.e. to the area towards $-\infty$ in the log scale. It is interesting to note that between the two expected extreme regions (respectively worst case (WC) and best-case (BC) regions) where SINR attains a floor (horizontal asymptotes), there exists a very large region, called intermediary or standard case (SC) region where the SINR variation in dB is asymptotically linear with a slope of 10dB per decade. Thus an asymptotic approximation of the empirical results can be written in closed form, also reported on fig. 5:

$$\text{SINR}_{\text{asympt}} = \begin{cases} n_r\text{SNR} & \text{if } |\cos(\theta)| \in [0, \frac{1}{2}] \quad \text{(BC)} \\ 2n_r\text{SNR}(1 - |\cos(\theta)|) & \text{if } |\cos(\theta)| \in [\frac{1}{2}, 1 - \epsilon] \quad \text{(SC)} \\ \text{SINR}_{\text{In}} & \text{if } |\cos(\theta)| \in [1 - \epsilon, 1] \quad \text{(WC)} \end{cases} \tag{10}$$

where $1 - \epsilon$ is the value of $\cos(\theta)$ corresponding to abscissa of the intersection point between the SC curve and the WC asymptote, resulting in $\epsilon = \text{SINR}_{\text{In}}/(2n_r\text{SNR})$. For e.g. in Fig. 4 with $P_I = 20$ dBm $\epsilon = 3.10^{-6}$, whereas when $P_I = 40$ dBm ϵ decreases to 3.10^{-8} due to the decrease of the WC asymptote. As demonstrated in the next subsection, this result gives an interesting insight about the small cell network case.

Small Cell Network Case

In this part, the consideration is moved to the multi-user model in a small cell network. This scenario is typically encountered in uncoordinated dense small networks, that are duplexed in time division (TDD) [11, 12]. A simple geometry based stochastic channel is used. Every signal passes through a single-path channel realization with a random angle of arrival uniform in $[-90°, 90°]$. The cell of interest is equipped by default with

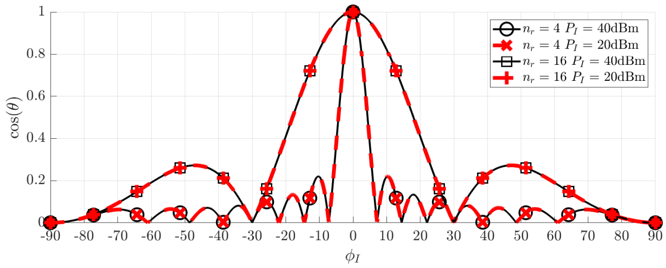

Fig. 3: Variation of $|\cos(\theta)|$ as a function of ϕ_I.

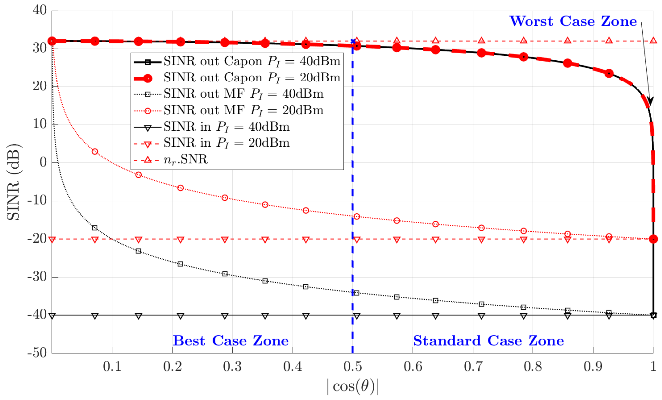

Fig. 4: Single-user single-interferer SINR as a function of $|\cos(\theta)|$ in linear scale.

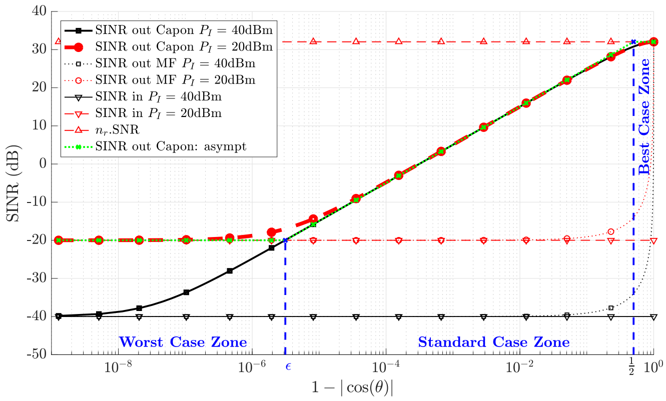

Fig. 5: Single-user single-interferer SINR as a function of $1 - |\cos(\theta)|$ in log scale. Asymptotes are shown only for $P_I = 20$ dBm.

$n_r = 16$ antennas, it receives $n_U = 4$ user signals of power 0 dBm. It operates thus in uplink. An adjacent small cell ($n_I = 1$) operates in downlink and interferes with the first small cell. Simulations are performed for $P_I = 20$ dBm. It is noted that from the perspective of a particular user, the other users behave as interferers, thus there are 4 interferers. Before investigating the SINR, first, the probability and the cumulative density functions (PDFs and CDFs respectively) of $|\cos(\theta)|$ are plotted in fig. 6 for various number of antennas. The uniform distribution of the angles of arrival conditions this parameter to be distributed over the values 0 and 1. However, on account of the CDFs it is observed that only a very little minority of the trials lead to WC region ($\cos(\theta) \in [1 - \epsilon, 1]$), and this phenomenon is further enhanced when the number of antennas increases, which is understood since the main lobe of the radiation pattern narrows (see Fig. 3). In Fig. 7 the bivariate histogram of the SINR and the high dimensional $\cos(\theta)$ are plotted. It can be seen that these two variables are tightly correlated and the SINR decreases as $\cos(\theta)$ increases. Fig. 8 shows the scatter-plot of the SINR and $1 - |\cos(\theta)|$ computed using 1000 channel realizations. A lower bound on the performance is clearly visible, and the extraction of the experimental lower bound shows (analogously to the single-user case) the three regions WC, SC and BC. This lower bound corresponds exactly to the single-user curve in Fig. 5. Thus it can be asymptotically approximated by the analytical SINR of eq. (10). The same observations stands in fig. 9 where the interference power is increased

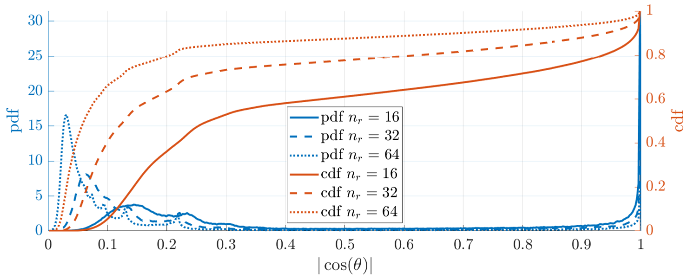

Fig. 6: $|\cos(\theta)|$ PDF and CDF for various number of antennas assuming uniformly distributed angles of arrivals.

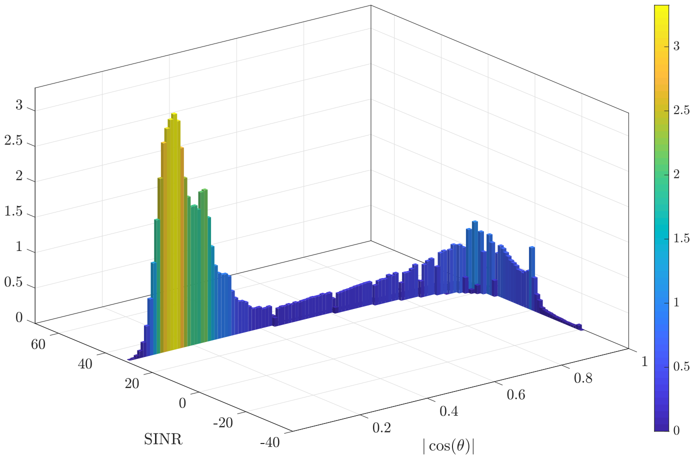

Fig. 7: SINR and $|\cos(\theta)|$ relative frequency histogram. $P_I = 20$dBm.

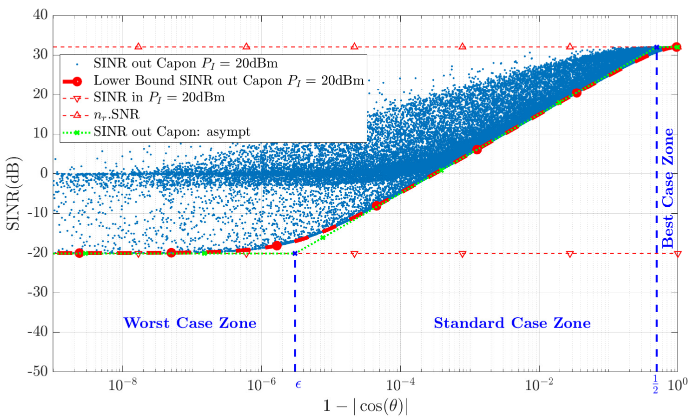

Fig. 8: Scatterplot of the SINR and $1 - |\cos(\theta)|$. $P_I = 20$ dBm.

to $Pi = 40$ dBm. This results in a decrease of the input SINR (lower asymptote in the WC zone) and an expansion of the linear SC zone. The BC zone remaining unchanged, as expected from the results of the previous section. The lower bound curve still corresponds to the single-user curve in fig. 5, with the appropriate value $P_I = 40$dBm. The aforementioned observations support the finding that the SINR lies in an area that can be asymptotically approximated by the eq. (10) of the single-user single-interferer case. This area is completely determined by the input SINR, the input SNR, the number of antennas and by the proposed macro-parameter $\cos(\theta)$, without the absolute necessity to know the exact micro-parameters (antenna channel responses, angles of arrival, etc.).

Conclusion: In this paper, a new parameter was introduced for interference characterization, consisting in the algebraic angle cosine between the user channel vector and the interferer channel vector in the single-user single-interferer case. This parameter is subsequently generalized in the multi-interferer case by using the algebraic angle between the user channel vector and the hyperplane generated by the interference channel matrix. In the case of Capon beamforming, this parameter conditions the SINR performance. In the single-user single-interferer case the SINR has 3 regimes, a worst case regime for sufficiently

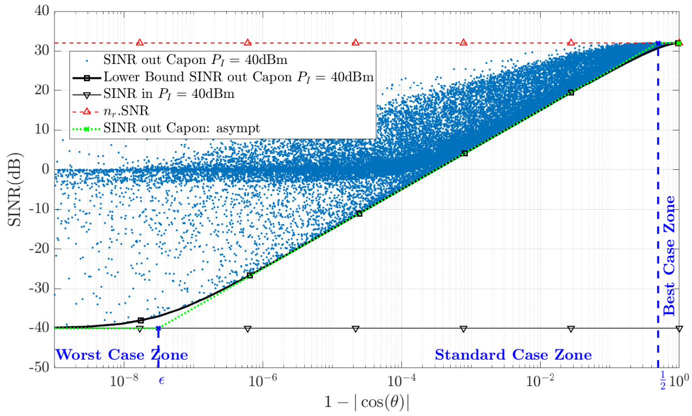

Fig. 9: Scatterplot of the SINR and $1 - |\cos(\theta)|$. $P_I = 40$ dBm.

high $|\cos(\theta)|$, a linear increase regime by 10 dB per decade of $1 - |\cos(\theta)|$, and the best case regime for sufficiently low $|\cos(\theta)|$. This single-user single-interferer case determines a lower bound on the SINR for the multi-user case with random distribution of angle of arrivals.

Acknowledgment: The authors thank Mohamed Sana at CEA-LETI for the fruitful given insights on MATLAB, and Sofia McGee-Renedo at CNRS-LNCMI for the constructive criticism of the manuscript.

M. R. Bekkar, S. Bories, B. Miscopein (*CEA-LETI, Minatec campus, Grenoble, France*)

M. R. Bekkar, L. Ros, C. Siclet (*Univ. Grenoble Alpes, CNRS, Grenoble INP (Institute of Engineering Univ. Grenoble Alpes), GIPSA-lab, 38000 Grenoble, France*)

E-mail: mohammed.reda.bekkar@gmail.com, laurent.ros@gipsa-lab.fr, cyrille.siclet@gipsa-lab.fr, serge.bories@cea.fr, benoit.miscopein@cea.fr.

References

1 M. Ding, D. Lopez-Perez, H. Claussen, and M. A. Kaafar, “On the fundamental characteristics of ultra-dense small cell networks,” *IEEE Network*, vol. 32, no. 3, pp. 92–100, 2018.

2 E. G. Larsson, O. Edfors, F. Tufvesson, and T. L. Marzetta, “Massive mimo for next generation wireless systems,” *IEEE Communications Magazine*, vol. 52, no. 2, pp. 186–195, February 2014.

3 J. Capon, “High-resolution frequency-wavenumber spectrum analysis,” *Proceedings of the IEEE*, vol. 57, no. 8, pp. 1408–1418, 1969.

4 S. M. Kogon, “Eigenvectors, diagonal loading and white noise gain constraints for robust adaptive beamforming,” in *The Thrity-Seventh Asilomar Conference on Signals, Systems & Computers, 2003*, vol. 2. IEEE, 2003, pp. 1853–1857.

5 Jian Li, P. Stoica, and Zhisong Wang, “On robust capon beamforming and diagonal loading,” *IEEE Transactions on Signal Processing*, vol. 51, no. 7, pp. 1702–1715, July 2003.

6 D. S. Baum, J. Hansen, J. Salo, G. Del Galdo, M. Milojevic, and P. Kyösti, “An interim channel model for beyond-3g systems: extending the 3gpp spatial channel model (scm),” in *2005 IEEE 61st Vehicular Technology Conference*, vol. 5, May 2005, pp. 3132–3136 Vol. 5.

7 S. Jaeckel, L. Raschkowski, K. Börner, and L. Thiele, “Quadriga: A 3-d multi-cell channel model with time evolution for enabling virtual field trials,” *IEEE Transactions on Antennas and Propagation*, vol. 62, no. 6, pp. 3242–3256, June 2014.

8 D. Tse and P. Viswanath, *Fundamentals of wireless communication*. Cambridge university press, 2005.

9 P. A. Wedin, “On angles between subspaces of a finite dimensional inner product space,” in *Matrix Pencils*, B. Kagstrom and A. Ruhe, Eds. Berlin, Heidelberg: Springer Berlin Heidelberg, 1983, pp. 263–285.

10 A. Bjorck and G. H. Golub, “Numerical methods for computing angles between linear subspaces,” *Mathematics of computation*, vol. 27, no. 123, pp. 579–594, 1973.

11 M. R. Bekkar, B. Miscopein, S. Bories, L. Ros, and C. Siclet, “Constant modulus hybrid beamforming for multi-user systems in the presence of blockers,” in *2018 25th International Conference on Telecommunications (ICT)*. IEEE, 2018, pp. 378–382.

12 M. Reda Bekkar, C. Siclet, L. Ros, B. Miscopein, and S. Bories, “On the use of semidefinite relaxation for uplink phase-only hybrid beamforming with blockers,” in *IEEE Wireless Communications and Networking Conference (WCNC 2019)*, Marrakech, Morocco, Apr. 2019.